Spin-resolved Compton scattering study of $RuSr_2GdCu_2O_8$

2005 J. Phys.: Condens. Matter 17 5533

(http://iopscience.iop.org/0953-8984/17/36/009)

INSTITUTE OF PHYSICS PUBLISHING JOURNAL OF PHYSICS: CONDENSED MATTER

J. Phys.: Condens. Matter **17** (2005) 5533–5540 doi:10.1088/0953-8984/17/36/009

Spin-resolved Compton scattering study of $RuSr_2GdCu_2O_8$

Z F Banfield[1], J A Duffy[1], J W Taylor[2], C A Steer[1], A Bebb[1], M J Cooper[1], L Blaauw[1], C Shenton-Taylor[1] and R Ruiz-Bustos[3]

[1] Department of Physics, University of Warwick, CV4 7AL, UK
[2] ISIS, RAL, Chiltern, Oxfordshire OX11 0QX, UK
[3] Inorganic Chemistry Laboratory of Oxford, South Parks Road, Oxford OX13 3QR, UK

Received 9 June 2005, in final form 4 August 2005
Published 26 August 2005
Online at stacks.iop.org/JPhysCM/17/5533

Abstract

The spin-polarized electron momentum distributions of the magnetic superconductor $RuSr_2GdCu_2O_8$ in its various phases have been measured using the magnetic Compton scattering technique with elliptically polarized synchrotron radiation. A contribution to the spin moment from magnetically ordered Ru 4d electrons was seen with a large induced Gd 4f moment below 25 K. A small negatively polarized component is observed in the antiferromagnetic phase of the Gd sublattice, at 2 K. The momentum distribution of this was consistent with the existence of a Gd 5d electron moment anti-parallel with respect to the now ordered Gd 4f moment.

1. Introduction

In this study magnetic Compton scattering has been used to investigate the bulk magnetic spin density in the Ru–O and Gd sublattices of $RuSr_2GdCu_2O_8$. We have identified and made quantitative analysis of the contributions to the spin moment from the Ru and Gd moments.

The ruthenate–cuprate compounds $RuSr_2RECu_2O_8$, (RE = Gd, Y, Eu), first synthesized by Bauernfeind *et al* [1] are currently of much interest because of their magnetic and superconducting properties. They exhibit the coexistence of magnetic order and superconductivity on a microscopic scale [2, 3] with, unusually, a magnetic ordering temperature much higher than the superconducting transition temperature. The structure is derived from the high-temperature superconductor $YBa_2Cu_3O_{7-d}$ (YBCO), in its orthorhombic form, in which the charge carriers travel in the CuO_2 planes. The yttrium is replaced by gadolinium and the CuO chain by a square planar RuO_2 layer, with resulting tetragonal symmetry except for small distortions typical of perovskites. The similarities in coordination and bond length in the CuO_2 and RuO_2 layers allow a range of structures. The system investigated in this paper is of the 1212-type consisting of CuO_2 bilayers and RuO_2 monolayers.

Spin-resolved or magnetic Compton scattering directly measures the spin-dependent electron momentum density distribution of a sample and isolates the spin moment. This

is the first measurement of the bulk spin moment of a sample in the $RuSr_2RECu_2O_8$ series and it offers an insight into the interplay of the Ru and rare earth moments in a system in which the magnetic properties are not yet fully understood. X-ray scattering is a particularly useful tool in this investigation as rare earths such as Gd are strong absorbers of neutrons. The magnetic Compton technique is especially suited to the study of Gd in a system as the 4f electrons are in a half-filled inner shell and so their distribution is not only isotropic but also well defined by free atom wavefunctions and thus easily identified in the Compton profile (see section 2).

In the Gd member of the series investigated here, the Ru moment orders magnetically at ∼133 K and there is a superconducting transition temperature at ∼35 K [3]. The Gd sublattice orders antiferromagnetically at ∼2.5 K, independent of the ordering in the Ru–O plane. The nature of the Ru moment's magnetic order is still debatable. Experimental results from various techniques have been interpreted as indicating a range of ordering types in the Ru–O plane. It was first thought to be ferromagnetic (FM) due to a rapid increase of magnetization with applied field [3], ferromagnetic resonance experiments [4] and a positive measurement of the Curie constant [5]. Neutron diffraction experiments then found superlattice reflections consistent with antiferromagnetic (AF) ordering for applied fields of up to ∼5 T, with the Ru moment aligned along the *c*-axis and neighbouring spins aligned anti-parallel [6]. From muon spin rotation and ferromagnetic resonance experiments the spins were found to be orientated in the *ab* plane. X-ray absorption spectroscopy experiments [7] and bond valence sum calculations [8] showed that the Ru ions are in a mixed valence state of 40% Ru^{4+} and 60% Ru^{5+} leading to the proposal of a double-exchange mechanism as explaining the contradictory FM and AF measurements [9].

Superconductivity is confined to the CuO_2 planes [10] and is highly dependent on the annealing temperature and other subtleties of the synthesis [11]. This is thought to be due to the oxygen non-stoichiometry causing vacancies on the RuO_2 plane which acts as a charge reservoir, doping the superconducting CuO_2 plane. An investigation of possible structural phase changes due to variables such as oxygen content and annealing temperature found no effect [12]. Direct current magnetization, muon spin rotation [3] and magnetic resonance experiments [4] have shown that the magnetic order is not significantly affected by the onset of superconductivity in the system [3]. Although the sample investigated here is not superconducting, the magnetic ordering temperatures are consistent with those from literature for superconducting samples, and the sample exhibits identical magnetic behaviour.

2. Magnetic Compton scattering

The Compton profile is defined as the one-dimensional projection of the electron momentum distribution, $n(\mathbf{p})$,

$$J(p_z) = \int\int n(\mathbf{p})\,\mathrm{d}p_x\,\mathrm{d}p_y, \tag{1}$$

and the integral of $J(p_z)$ is conventionally taken as the total number of electrons per formula unit. The profile is obtained experimentally by the inelastic scattering of mono-energetic photons through a fixed angle. The scattered photon energy is Doppler broadened into an energy distribution by the momenta of the electrons. This distribution is directly related to the Compton profile through the double differential scattering cross section [13].

If the photons have a component of circular polarization then a small spin-dependent term appears in the scattering cross section. Changing either the polarization of the photons or the direction of the sample's magnetization changes the sign of this spin-dependent term. In the latter method, adopted here, this term is isolated by taking the difference of two Compton

profiles obtained with the magnetic field parallel and anti-parallel to the z-direction to give a magnetic Compton profile (MCP),

$$J_{\mathrm{mag}}(p_z) = \int\int [n\uparrow(\mathbf{p}) - n\downarrow(\mathbf{p})]\,\mathrm{d}p_x\,\mathrm{d}p_y \tag{2}$$

where $n\uparrow(\mathbf{p})$ and $n\downarrow(\mathbf{p})$ are the momentum-dependent spin densities for the majority and minority bands respectively. This is the projection of the momentum density of only those electrons with unpaired spins and the area under the MCP is equal to the number of unpaired electrons, i.e. the spin momentum per formula unit. If the scattering is within the impulse approximation [14] as is invariably the case, the spin moment but not the orbital moment of the sample is measured [15–17].

Relativistic Hartree–Fock (RHF) free atom profiles were used to compare the experimental MCPs to theory. Free atom MCPs based on RHF equations can be calculated by Fourier transforming the position space wavefunction [18]. By adding or subtracting the relevant shell-specific lineshapes, free atom profiling can be used to decompose experimentally obtained MCPs into shell and site specific contributions [19]. RHF free atom profiles accurately describe isotropic inner shell electrons, an excellent example being the half-filled Gd 4f shell. Whilst the momentum density of more delocalized electron bands can only be accurately modelled using electronic band structure calculations, the overall momentum width of the contributions to the spin moment obtained should be unchanged from those predicted by RHF free atom profiles. On this premise, RHF free atom profiles can be used as a theoretical comparison for 4d and 5d electron spin moments as demonstrated in previous magnetic Compton studies [19–21].

3. Experimental details

Polycrystalline samples of $RuSr_2GdCu_2O_8$ were synthesized by solid-state reaction of stoichiometric powders of RuO_2, $SrCO_3$, Gd_2O_3 and CuO_2. The RuO_2, $SrCO_3$, Gd_2O_3 were calcined in air at 1250 °C for 4 days, being ground, milled and die-pressed into pellets every 24 h to prepare the precursor Sr_2GdRuO_6. This was then sintered with CuO_2 at 1050 °C under oxygen for 7 days to obtain $RuSr_2GdCu_2O_8$. The sample was then allowed to cool to room temperature in an oxygen flow.

Magnetization measurements were carried out on a SQUID with magnetic fields up to 6 T and temperatures down to 2 K. The data, in figure 1, show an upturn in magnetization at ∼35 K but show no evidence of a diamagnetic response, which would indicate a transition to a superconducting state. Although our sample is not superconducting the magnetic transition temperatures, T_{M}(Ru–O) = 130±1 K and T_{M}(Gd) = 3.0±0.3 K, agree with published results of T_{M} (Ru–O) of values from ∼130 to 136 K and T_{M}(Gd) = 2.5 ± 1.0 K. We conclude that the magnetic structure of the sample is unchanged from that of stoichiometric $RuSr_2GdCu_2O_8$ despite the absence of superconductivity.

The MCPs were measured on the high-energy x-ray beamline (ID15) at the ESRF, Grenoble. The experiment was performed in a reflection geometry with an incident beam energy of 200 keV, obtained using the {220} reflection of a Si monochromator and a scattering angle of 172°. The temperature of the sample was controlled to ±1 K and measurements were taken between 2 and 100 K. The sample's magnetization was periodically reversed with a 0.96 T electromagnet. The energy distribution of the scattered x-rays was measured by a 13-element solid state Ge detector. The momentum resolution, of 0.44 atomic units (au, where 1 au = 1.99×10^{-24} kg m s^{-1}), is determined by the detector collimation, the source divergence and the intrinsic resolution of the detector, the last being dominant. This resolution is typical for the magnetic Compton scattering technique in recent years and has been shown to be adequate

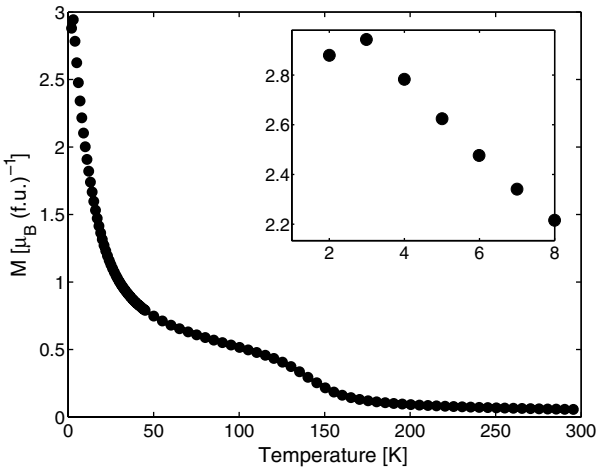

Figure 1. SQUID magnetization data as a function of temperature of $RuSr_2GdCu_2O_8$ in a 1 T field. The inset shows a magnification of the low-temperature region.

for quantitative analysis of experimental MCPs [16, 22, 23]. The data were corrected for the energy dependence of the detector efficiency, sample absorption and the relativistic scattering cross section. After checking that the data were symmetrical they were folded about zero momentum to increase the effective statistics. The MCPs were normalized to magnetization data at 2 K rather than being normalized onto an absolute scale by comparison to Ni (the usual 'standard' ferromagnet used for calibration), as the effect of background scattering on the measurement of the sample and that of Ni is different. This background scattering is seen only in the charge profile, and so has no effect on the shape of the MCP, but it causes a slightly increased value of the spin moment. On the other hand the comparison of spin moments at different temperatures is unaffected by the normalization technique. It is reasonable to assume that the orbital contribution to the total moment is negligible in this system, as Gd has no orbital moment and any Ru 4d electron orbital moment would be quenched due to the delocalization of these electrons, as is the case with transition metal 3d electrons.

4. Magnetic Compton scattering results and discussion

Figure 2(a) shows the experimental MCPs at 2 and 8 K with the RHF free atom fits to the 8 K data. At both temperatures the data are consistent with a large Gd 4f moment, exclusively responsible for the shape of the profiles in the high momentum region, i.e. above 4 au. This is as expected, since the other likely contributions to the spin-polarized momentum density will not contribute at these momenta. Because the electrons in the half-filled 4f shell are well localized, the RHF free atom calculation is likely to be an accurate model: indeed previous work, such as in pure Gd [24], has always shown this to be the case. Below 4 au, it can be seen that there is an additional contribution to the moment which is different for the 2 and 8 K data. The data at 8 K can be successfully fitted by the addition of a Ru 4d moment, as seen in figure 2(a).

The MCP at 2 K shows a dip at a low momentum ($p_z \sim 0.6$ au) indicative of a negatively polarized contribution to the spin moment not seen above the Gd sublattice ordering temperature, at 8 K. This feature can best be fitted by adding a negatively polarized Gd 5d moment to the model for the 8 K data with an enhanced Ru 4d moment, discussed quantitatively

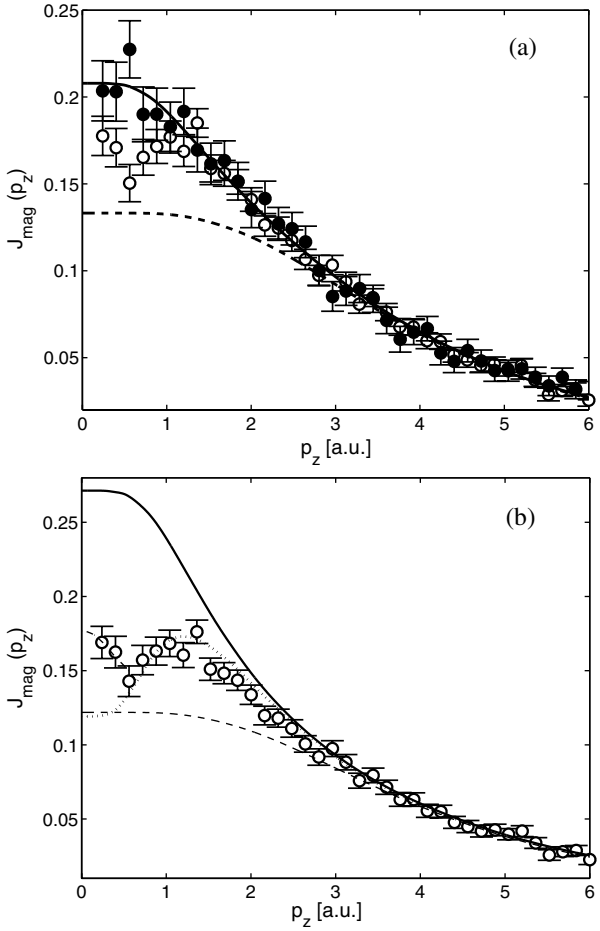

Figure 2. (a) MCPs of $RuSr_2GdCu_2O_8$ at 2 K (○) and 8 K (●), folded about zero momentum and with a momentum scale bin width of 0.2 au, are shown. RHF free atom fits of a Gd 4f moment (- - - -) and a combination of this Gd 4f moment and a Ru 4d moment which describes the 8 K profile within experimental error (——) are plotted. (b) The MCP of $RuSr_2GdCu_2O_8$ at 2 K (○), folded about zero momentum and with a momentum scale bin width of 0.2 au, is shown. RHF free atom fits of a Gd 4f moment (- - - -), and a combination of this Gd 4f moment and an enhanced Ru 4d moment with respect to that in the fit of the data at 8 K (——) are plotted. In order to model the dip in the data, a negatively polarized Gd 5d moment has been added (· · · · · ·), producing a fit to the data down to ∼0.6 au. The rise from 0.6 to 0 au is fitted by adding a delocalized electron contribution modelled as a free electron gas of Fermi momentum 0.65 au.

later. These contributions combine to produce a dip consistent with the experimental data, as shown in figure 2(b). This model has a sound theoretical basis, as anti-parallel ordering of the Gd 5d and 4f electron moment has been observed in other systems with the onset of antiferromagnetism [25]. The use of the free atom model for this material is a first approximation but is the only theoretical model available to us at this time, band structure calculations being difficult in such a complex structure. Whilst the shape of theoretical profiles produced from band structure calculations would be in principle different, the momentum region occupied by the various contributions would be very similar. Considering the limited momentum resolution and statistical accuracy of the data, the main features predicted by the

Table 1. Magnetic moments, in Bohr magnetons per formula unit $\mu_B(\text{f.u.})^{-1}$, of $RuSr_2GdCu_2O_8$ as a function of temperature. The table lists the spin moments deduced from the Compton data normalized at 2 K to the total moments from SQUID data and the electronic contributions to the spin moment estimated from RHF free atom fits of MCPs within the experimental error bars.

Temperature (K)	Spin moment $\mu_B(\text{f.u.})^{-1}$	Total moment $\mu_B(\text{f.u.})^{-1}$	Estimated Gd 4f spin moment $\mu_B(\text{f.u.})^{-1}$	Estimated Ru 4d spin moment $\mu_B(\text{f.u.})^{-1}$	Estimated Gd 5d spin moment $\mu_B(\text{f.u.})^{-1}$	Estimated conduction electron spin moment $\mu_B(\text{f.u.})^{-1}$
2	2.9 ± 0.2	2.88 ± 0.01	2.1 ± 0.3	1.0 ± 0.3	-0.65 ± 0.05	0.10 ± 0.01
8	2.5 ± 0.3	2.21 ± 0.01	2.0 ± 0.2	0.5 ± 0.1	—	—
25	1.4 ± 0.3	1.13 ± 0.01	1.0 ± 0.2	0.4 ± 0.1	—	—
100	0.8 ± 0.4	0.52 ± 0.01	0.5 ± 0.2	0.3 ± 0.2	—	—

free atom model and band calculations will be in practice little different, making this simple model a useful first analysis of the data.

The rise of the profile below 0.6 au can be fitted using a delocalized electron moment which could originate from hybridization of the Gd 6s electron band. The contribution of delocalized electrons is modelled by projecting the free electron density distribution onto the one-dimensional MCP momentum scale giving a parabola with the origin at zero momentum and width dependent on the Fermi momentum. The parabola used in this fit has a full width of 0.65 ± 0.03 au corresponding to a real space electron gas delocalized over 2.9 ± 0.1 Å, the error estimated from the MCP data points. Again, the use of the free electron model is a first approximation in this case: a more detailed analysis would require a band structure calculation.

5. Spin moment analysis

Fitting the MCPs measured at 25 and 100 K by the same method allows quantitative study of the electron spin moment contributions with temperature, as shown in table 1. The errors are estimated from the MCP data points. There is a large contribution to the spin moment from an induced Gd 4f moment, increasing on cooling to $2.1 \pm 0.3\ \mu_B$ per formula unit, $(\text{f.u.})^{-1}$, at 2 K where a Gd 5d moment estimated as $-0.65 \pm 0.05\ \mu_B(\text{f.u.})^{-1}$, ∼30% of the Gd 4f moment, is seen. The delocalized electron moment at 2 K is estimated as $0.10 \pm 0.01\ \mu_B(\text{f.u.})^{-1}$, and is not present at higher temperatures. On cooling, the Ru 4d moment remains low, $0.4 \pm 0.2\ \mu_B(\text{f.u.})^{-1}$, until below 8 K where it rises sharply to $1.0 \pm 0.3\ \mu_B(\text{f.u.})^{-1}$. This increase in the Ru 4d moment could be due to the onset of another magnetic ordering phase in this temperature region; however, the magnetization data show no indication of this. It is more likely that the Ru 4d electron moment increase is associated with the AF ordering of the Gd, perhaps by hybridization with Gd 5d or 6s electrons.

In discussing these results we note that it is possible that our free atom model overestimates both the Gd 5d and Ru 4d moments at 2 K, and the apparent increase in the Ru 4d moment described may arise from the fitting procedure used. To account for the shape of the experimental profile, the Gd 5d moment is correlated to the value of the Ru 4d moment: hence the Gd 5d moment could also be slightly smaller than calculated here. Lesser magnitude RHF free atom fits produce dips at similar momentum values but do not fit the MCP within experimental error. Band structure calculations would give a more accurate profile *shape* with which to fit the data and therefore the estimated magnitudes of the contributions would differ. The *width* of the theoretical profile, however, would not differ significantly. We emphasize

that some negative polarized moment is required at 2 K, because of the dip in the profile, and that the momentum distribution of this dip is distinctly characteristic of that which would be expected from a negatively polarized Gd 5d electron moment.

The Gd 5d and Ru 4d moment should be investigated further using x-ray magnetic circular dichroism as the energy can be tuned to the relevant binding energies and identify any hybridization between electron bands. This would be helpful in establishing the origin of the delocalized electron moment and any hybridization with Ru 4d electrons. Although the analysis would be difficult due to the complicated structure, a relative measurement over the temperature region of the Gd sublattice ordering would be sufficient to determine if there is any correlation of the moment with this ordering phase.

6. Conclusion

In conclusion, the obtained magnetic Compton profiles allow us to determine that the spin moment of $RuSr_2GdCu_2O_8$ is made up of a large induced Gd 4f electron moment with a contribution from magnetically ordered Ru 4d electrons at 8 K and above. More interestingly, a negatively polarized component was observed at 2 K, below the Gd sublattice ordering temperature of 3.0 ± 0.3 K. Using relativistic Hartree–Fock free atom wavefunctions we have successfully modelled this feature using a Gd 5d electron spin moment, of $0.65 \pm 0.05\ \mu_B(\text{f.u.})^{-1}$, aligned anti-parallel with respect to that of the Gd 4f electron moment. It has been suggested that this behaviour in other systems is related to the onset of antiferromagnetism in Gd atoms and so this observation supports theories that the Gd sublattice order is indeed antiferromagnetic. An enhanced Ru 4d electron moment of $1.0 \pm 0.3\ \mu_B(\text{f.u.})^{-1}$ is seen at 2 K which we propose is correlated to the Gd ordering, possibly due to hybridization with Gd 5d or 6s electrons. A delocalized electron moment of magnitude of $0.10 \pm 0.01\ \mu_B(\text{f.u.})^{-1}$, which could originate from a hybridized Gd 6s electron band, was also seen at 2 K. Given that the existence of the apparent Ru 4d enhancement and the 'delocalized' moment are deduced from a free atom fit, full band structure calculations would be worthwhile to investigate this compound further.

Although the estimated magnitudes of the Gd 5d and Ru 4d moments at 2 K are model dependent, the dip in the magnetic Compton lineshape is an unambiguous indicator of a negative (antiferromagnetically coupled) contribution. Furthermore, only Gd 5d electrons have the characteristic momentum density distribution corresponding to that of the observed negative contribution.

Acknowledgments

We would like to thank the ESRF for allocation of beamtime, and the University of Warwick Superconductivity and Magnetism Group for assistance and expertise. We thank the EPSRC and JAD thanks the Nuffield Foundation (Grant reference: NAL/00428/G) for generous financial support.

References

[1] Bauernfeind L, Widder W and Braun H F 1996 *J. Low Temp. Phys.* **105** 1605
[2] Tallon J, Bernhard C, Bowden M, Gilberd P, Stoto T and Pringle D 1999 *IEEE Trans. Appl. Supercond.* **9** 2
[3] Bernhard C, Tallon J L, Niedermayer Ch, Blasius Th, Golnik A, Brücher E, Kremer R K, Noakes D R, Stronach C E and Ansaldo E J 1999 *Phys. Rev.* B **59** 14099
[4] Fainstein A, Winkler E and Tallon J 2001 *Phys. Rev.* B **60** R12597

[5] Butera A, Fainstein A, Winkler E and Tallon J 2001 *Phys. Rev.* B **63** 054442
[6] Lynn J W, Keimer B, Ulrich C, Bernhard C and Tallon J L 2000 *Phys. Rev.* B **61** R14964
[7] Liu R S, Jang L Y, Hung H H and Tallon J L 2001 *Phys. Rev.* B **63** 212507
[8] McLaughlin A C, Zhou W, Attfield J P, Fitch A N and Tallon J L 1999 *Phys. Rev.* B **60** 7512
[9] Aliaga H and Aligia A A 2002 *Physica* B **320** 34
[10] Požek M, Dulčić A, Paar D, Hamzić A, Basletić M, Tafra E, Williams G V M and Krämer S 2002 *Phys. Rev.* B **65** 174514
[11] Lorenz B, Meng R L, Cmaidalka J, Wang Y S, Lenzi J, Xue Y Y and Chu C W 2001 *Physica* C **363** 251
[12] Cordero F, Ferretti M, Cimberle M R and Masini R 2003 *Phys. Rev.* B **67** 144519
[13] Holm P 1988 *Phys. Rev.* A **37** 3706
[14] Platzman P M and Tzoar N 1970 *Phys. Rev.* B **2** 3556
[15] Sakai N 1996 *J. Appl. Crystallogr.* **29** 81
[16] Cooper M J, Mijnarends P E, Shiotani N, Sakai N and Bansil A 2004 *X-Ray Compton Scattering* (Oxford: Oxford University Press)
[17] Lovesey S W 1996 *J. Phys.: Condens. Matter* **8** L353
[18] Biggs F, Mendelsohn L B and Mann J B 1975 *At. Data Nucl. Data Tables* **16** 201
[19] Cooper M J, Lawson P K, Dixon M A G, Zukowski E, Timms D N, Itoh F, Sakurai H, Katawa H, Tanaka Y and Ito M 1996 *Phys. Rev.* B **54** 4068
[20] Lawson P K, Cooper M J, Dixon M A G, Zukowski E, Timms D N, Itoh F, Sakurai H, Kawata H, Tanaka Y and Ito M 1997 *Phys. Rev.* B **56** 3239
[21] Lawson P K, McCarthy J E, Cooper M J, Timms D N, Zukowski E, Itoh F, Sakurai H, Tanaka Y, Kawata H and Ito M 1995 *J. Phys.: Condens. Matter* **7** 389
[22] Bebb A M, Taylor J W, Duffy J A, Banfield Z F, Cooper M J, Lees M R, McCarthy J E and Timms D N 2005 *Phys. Rev.* B **71** 024407
[23] Taylor J W, Duffy J A, Bebb A M, McCarthy J E, Lees M R, Cooper M J and Timms D N 2002 *Phys. Rev.* B **65** 224408
[24] Duffy J A, McCarthy J E, Dugdale S B, Honkimaki V, Cooper M J, Alam M A, Jarlborg T and Palmer S B 1998 *J. Phys.: Condens. Matter* **10** 10391
[25] Okuyama D, Matsumura T, Murakami Y, Wakabayashi Y, Sawa H and Li D X 2003 *Physica* B **345** 63